

# Gas-Phase Basicities and Acidities of Ethyl-, Vinyl-, and Ethynylarsine. An Experimental and Theoretical Study

Jean-Claude Guillemin\*

Laboratoire de Synthèse et Activation de Biomolécules, ESA 6052, ENSCR, 35700 Rennes Cedex, France

Michèle Decouzon, Pierre-Charles Maria, and Jean-François Gal\*

Groupe FT-ICR, Laboratoire de Chimie Physique Organique, Université de Nice-Sophia Antipolis, Parc Valrose, 06108 Nice Cedex, France

Otilia Mó and Manuel Yáñez\*

Departamento de Química, C-9, Universidad Autónoma de Madrid, Cantoblanco, 28049 Madrid, Spain

Received: July 24, 1997; In Final Form: September 16, 1997<sup>®</sup>

The gas-phase basicities and acidities of ethynyl-, vinyl- (or ethenyl-), and ethylarsine have been measured by means of FT-ICR techniques. The structures of the different neutral, protonated, and deprotonated species were elucidated by means of ab initio molecular orbital calculations at the MP2 level. Their final energies were calculated in the framework of the G2 theory. The agreement between calculated and experimental values for both basicities and acidities was fairly good. Protonation of vinylarsine and ethynylarsine at the C<sub>α</sub> carbon leads to the breaking of the C–As bond, such that the corresponding protonated species can be viewed as complexes between ethylene and acetylene, respectively, with a AsH<sub>2</sub><sup>+</sup> cation. More importantly, these complexes are predicted to be as stable as the cations formed by direct protonation at the arsenic atom. For the particular case of ethynylarsine, this result is consistent with the experimental evidence. The gas-phase basicity decreases (*GB* values decrease) and acidity increases ( $\Delta_{\text{acid}}G^\circ$  values decrease) in the following order: ethylarsine, vinylarsine, ethynylarsine. The performance of the B3LYP density functional approach in the description of the thermochemical properties of these arsenic-containing species was also studied.

## Introduction

Although the thermochemistry of compounds containing third-row elements, especially the third-row hydrides, has received particular attention in recent years,<sup>1–3</sup> information on the intrinsic basicities and acidities of these compounds is very scarce. Only recently have the experimental gas-phase acidities or basicities of GeH<sub>4</sub>, AsH<sub>3</sub>, SeH<sub>2</sub>, and HBr been reported in the literature.<sup>4–7</sup>

In this paper we report the gas-phase basicities and the gas-phase acidities of the arsine series, ethynylarsine, vinylarsine (or ethenylarsine) and ethylarsine, with the aim of studying the interaction between the arsine function and an unsaturated system. Compounds bearing the simplest vinyl and ethynyl unsaturated groups, and ethyl, their corresponding saturated substituent for comparison, are amenable to high level ab initio calculations thereby allowing the characterization of the most stable protonated and deprotonated species. Since the theoretical information on arsenic derivatives is very scarce,<sup>7,8</sup> we have considered it of interest to investigate the performance of the B3LYP density functional approach, which has been shown to provide reliable gas-phase proton affinities for bases containing first- and second-row atoms.<sup>9–11</sup>

## Experimental Section

**Safety Considerations.** Arsines are potentially highly toxic compounds. All reactions and handling should be carried out in a well-ventilated hood.

**Chemicals.** Vinyl- and ethynylarsines were prepared by the reduction of the corresponding dichloroarsines with Bu<sub>3</sub>SnH,

as previously described.<sup>12,13</sup> Dichloroethylarsine was prepared in 93% yield by addition of 1 equiv of diethylmercury to 1 equiv of arsenic chloride and purified by distillation (bp 153 °C at atmospheric pressure). Its reduction into ethylarsine was carried out with Bu<sub>3</sub>SnH using a similar experimental procedure as for the  $\alpha$ -unsaturated arsines (yield 80%). All the compounds were purified in a vacuum line by trap-to-trap distillation. At a pressure of 10 Pa, the high boiling impurities were selectively removed in a trap cooled at –100 °C and the substituted arsine was condensed in a trap cooled at –120 °C. The most volatile impurities (mainly AsH<sub>3</sub>) were not condensed at –120 °C and thus removed. The cell containing the expected arsine, isolated from the vacuum line by stopcocks, was directly fitted to the inlet system of the FT-ICR mass spectrometer.

The compounds used as references for the gas-phase basicity and acidity determinations are of the highest purity commercially available. They were used without further purification, except several freeze, pump, thaw cycles in the spectrometer inlet system.

**FT-ICR Measurements.** Proton-transfer equilibrium measurements were conducted on an electromagnet Fourier transform ion cyclotron resonance (FT-ICR) mass spectrometer built at the University of Nice-Sophia Antipolis, using the methodology described previously.<sup>14–16</sup> Variable pressure ratios between the unknown base or acid under study and the reference compound, differing by at least a factor of 3, were used, with total pressures in the range  $2 \times 10^{-5}$  to  $8 \times 10^{-5}$  Pa (as read on a Bayard Alpert ion gauge). Relative (to N<sub>2</sub>) sensitivities *S<sub>r</sub>* of the Bayard Alpert gauge have been estimated using the Bartmess and Georgiadis equation:<sup>17</sup>

<sup>®</sup> Abstract published in *Advance ACS Abstracts*, November 15, 1997.

$$S_r = 0.36 \alpha + 0.30 \quad (1)$$

The molecular polarizability  $\alpha$  was taken as  $\alpha(\text{ahc})$ , calculated using the atomic hybrid component ( $\tau$ ) approach of Miller.<sup>18</sup>  $\tau$  value for arsenic was not available and thus required calculation ( $\tau_{\text{As}} = 5.807 \text{ \AA}^3/2$ ) from  $S_r(\text{AsH}_3) = 2.12 \pm 0.01$ ; a value experimentally determined in Nice, using a spinning rotor gauge.<sup>19</sup>

For basicity determinations, proton-transfer reactions were followed for 5–10 s after a 70 eV electron ionization pulse. For ethynylarsine, we observed a fast decomposition of the protonated molecule, and equilibrium conditions could not be reached. Consequently, bracketing experiments were carried out. A mixture of the neutral base and the chosen reference was ionized and allowed to react for 0.3 to 1 s. The ion of interest, either the protonated base or the protonated reference, was isolated by broad band RF resonant ejection. The occurrence of proton transfer was then checked by allowing the ion to react for 0.5 to 2 s with the neutral partner.

For acidity determinations, negative ions were generated by proton abstraction from the neutral reactant by t-BuO<sup>-</sup>. This anion was obtained via electron ionization at 0.1 eV (nominal) of t-BuONO, introduced in the spectrometer at a partial pressure of about  $10^{-5}$  Pa. The proton-transfer reactions were monitored for about 10 s without the manifestation of significant secondary reactions.

### Computational Details

The theoretical treatment of the different systems included in this work was performed by using the Gaussian-94 series of programs.<sup>20</sup> Initially, the geometries of the different neutral and protonated species investigated were optimized at the HF/6-31G\* level.<sup>21</sup> These geometries were then refined at the MP2/6-31G\* level which explicitly took into account electron-correlation effects. To investigate the performance of density-functional approaches, the geometries of neutral and protonated species were also optimized using the B3LYP method with an 6-311G(d) expansion. The B3LYP approach is a hybrid method which combines the Becke's three-parameter nonlocal exchange potential<sup>22</sup> with non local correlation functional of Lee, Yang, and Parr.<sup>23</sup> The geometry optimization of the corresponding anionic species was carried out at the B3LYP/6-311+G(d,p) level, since it has been well established that the basis set used to describe anionic species must incorporate diffuse components.<sup>24</sup> The corresponding harmonic vibrational frequencies were calculated at the same level of theory used for the geometry optimizations. This allowed us to state conclusively that the stationary points found were indeed local minima of the potential energy surface and to calculate both the corresponding zero point energies (ZPE) and entropies. ZPEs calculated at the HF/6-31G\* level were scaled by the empirical factor of 0.893. For those obtained at the B3LYP level, the 0.98 empirical factor proposed by Bauschlicher<sup>25</sup> was used.

To obtain reliable final energies we have used the G2 theory,<sup>21,26</sup> which has been shown to provide thermodynamical properties within chemical accuracy (0.1 eV) and has been recently extended to third-row atoms.<sup>21</sup> Since calculations on As containing systems are very scarce we have considered it of interest to compare the performance of the B3LYP approach with the aforementioned high-level ab initio calculations. Hence, the final energies of the different species under consideration were also calculated at the B3LYP/6-311+G(3df,-2p) level using the B3LYP optimized geometries. This theoretical scheme has been found to provide protonation energies in good agreement with experimental values and with estimates obtained using high-level ab initio techniques in the framework

**TABLE 1: Gas-Phase Basicities in kcal mol<sup>-1</sup> from Proton-Transfer Equilibrium Constant Determinations or Bracketing Experiments**

B	ref	GB(ref) <sup>a</sup>	$\Delta GB(338 \text{ K})^b$	GB(B) <sup>c</sup>
ethylarsine	Me <sub>2</sub> CO	186.9	+0.14 ± 0.10	187.2 ± 0.2
	t-BuSH	187.6	-0.19 ± 0.02	
vinylarsine	n-PrCHO	181.8	+1.63 ± 0.14	183.6 ± 0.2
	n-BuCHO	183.1	+0.60 ± 0.02	
	n-PrCN	183.9	-0.17 ± 0.02	
ethynylarsine	ClCH <sub>2</sub> CN	170.9	d	175.2 ± 2.4 <sup>e</sup>
	CF <sub>3</sub> CO <sub>2</sub> Et	174.1	≤ 0	
	MeCHO	176.2	≤ 0	
	MeCN	178.8	< 0	
	HCO <sub>2</sub> Me	179.8	< 0	
	n-PrCHO	181.8	< 0	

<sup>a</sup> Absolute gas-phase basicities (Gibbs energies at 298.15 K for the reaction  $\text{RefH}^+ \rightarrow \text{Ref} + \text{H}^+$ ) from ref 27. <sup>b</sup> Gibbs energies for the reaction:  $\text{BH}^+ + \text{Ref} \rightarrow \text{RefH}^+ + \text{B}$ ; quoted uncertainties correspond to the standard deviation for three to four measurements. <sup>c</sup> Absolute gas-phase basicities; no temperature correction applied, see text; for equilibrium determinations, quoted uncertainties correspond to the overlap quality. <sup>d</sup> Not conclusive; reactions other than proton-transfer dominate. <sup>e</sup> Unstable or reactive  $\text{BH}^+$  ions; experimental uncertainties estimated from the range of reference-compounds basicities used in the equilibrium or bracketing experiments.

of the G2 theory, for bases containing first-row and second-row atoms.<sup>9–11</sup>

We have also considered it of interest to investigate the effect of using B3LYP optimized geometries rather than the MP2 ones in our G2 calculations. This approach will be denoted hereafter as G2/DFT.

### Results and Discussion

**Experimental Basicities and Acidities.** Results of the equilibrium-constant basicity determinations and the bracketing experiments are presented in Table 1. Absolute gas-phase basicities  $GB$ s of reference compounds were taken from the recent gas-phase ion energetics data compilation of Hunter and Lias.<sup>27</sup> Data on positive ions, in particular  $GB$ s and proton affinities  $PA$ s, are available on the NIST Internet server. Differences greater than 2 kcal mol<sup>-1</sup> between  $GB$ s reported in this compilation and those given in the published version<sup>28</sup> were noted. For ethyl- and vinylarsine, equilibrium measurements against different reference compounds were self-consistent as reflected by the indicated uncertainties. These uncertainties are useful for estimating the precision of differences in basicity, but the accuracy of the absolute  $GB(B)$  is linked to the accuracy of the reference scale. Indeed, the NIST scale<sup>27,28</sup> is still evolving. Secondary reactions, competing with proton transfer between the neutral bases, made equilibrium-constant determinations for ethynylarsine impossible. During the measurements, we observed the formation of ionic species containing two to four arsenic atoms. In this case  $GB$  was obtained by bracketing, leading to a large uncertainty. Equilibrium constants were obtained with a ICR cell temperature of 338 K. Tabulated  $GB$ s refer to the standard temperature of 298.15 K.<sup>27</sup> Temperature corrections of the relative gas-phase basicities  $\Delta GB$ s from 338 to 298 K, which necessitate an estimation of the entropy change associated with proton exchange,<sup>6</sup> are difficult in the present study, in particular because of the uncertainty regarding the site of protonation, vide infra. Such corrections are probably minor as regard to other experimental uncertainties.

Acidities are reported in Table 2. Absolute gas-phase acidities have been referred to the NIST Negative Ion Energetics Database.<sup>29</sup> For the reasons given above concerning basicity determinations, no temperature corrections were applied. Uncertainties (0.1–0.2 kcal mol<sup>-1</sup>) given for  $\Delta_{\text{acid}}G^\circ(\text{AH})$  are in line with the precision (0.1–0.3 kcal mol<sup>-1</sup>) reported by

**TABLE 2: Gas-Phase Acidities in kcal mol<sup>-1</sup> from Proton-Transfer Equilibrium Constant Determinations**

AH	RefH	$\Delta_{\text{acid}}G^{\circ}$ - (RefH) <sup>a</sup>	$\Delta\Delta_{\text{acid}}G^{\circ}$ - (338 K) <sup>b</sup>	$\Delta_{\text{acid}}G^{\circ}$ - (AH) <sup>c</sup>
ethylarsine	CH <sub>2</sub> =CHCOMe	356.5	≈+0.9	
	EtCHO	358.7	-0.03 ± 0.2	358.7 ± 0.1
vinylarsine	MeCHO	359.0	-0.24 ± 0.11	
	H <sub>2</sub> S	344.8	+1.41 ± 0.06	
	t-BuSH	346.2	-0.34 ± 0.10	
ethynylarsine	EtSH	348.9	-2.66 ± 0.01	346.1 ± 0.2
	CF <sub>3</sub> COMe	342.1	+0.53 ± 0.05	
	H <sub>2</sub> S	344.8	-1.90 ± 0.10	342.7 ± 0.2

<sup>a</sup> Absolute gas-phase acidities (Gibbs energies at 298.15 K for the reaction: RefH → Ref<sup>-</sup> + H<sup>+</sup>) from ref 29. <sup>b</sup> Gibbs energies for the reaction: AH + Ref<sup>-</sup> → A<sup>-</sup> + RefH; quoted uncertainties correspond to the standard deviation for three to four measurements. <sup>c</sup> Absolute gas-phase acidities; no temperature correction applied, see text; for equilibrium determinations, quoted uncertainties correspond to the overlap quality.

Bartmess for relative acidities.<sup>29</sup> However, errors on these absolute acidities are estimated to be about 10 times larger (2–3 kcal mol<sup>-1</sup>) due to the uncertainties associated with absolute  $\Delta_{\text{acid}}G^{\circ}$ (RefH) values.<sup>29</sup> These larger errors must be kept in mind when comparisons are made with ab initio results.

An increase in the degree of unsaturation of the substituent on going from ethyl to ethynyl induces a decrease in basicity (*GB* values decrease) and conversely induces an increase in acidity ( $\Delta_{\text{acid}}G^{\circ}$  values decrease). These sequences suggest that the main effect governing these properties is electronegativity or field/inductive effect,<sup>30</sup> if we suppose that protonation and deprotonation occur at the arsenic atom. Indeed, polarizability effect is minimized, the three substituents having close  $\sigma_{\alpha}$  values,<sup>30</sup> and resonance effect, if dominant, would not induce the observed order. However, these unsaturated arsines possess more than one potential site of protonation or deprotonation. For example, ethylenes with electron-donor heteroatoms are protonated on the carbon  $\beta$  to the heteroatom.<sup>31–33</sup> On the other hand, acetylenic C–H may be sufficiently acidic to compete with As–H. Therefore, we undertook a detailed ab initio study on the structure and energetics of the neutral molecules and the isomeric ions corresponding to the protonation and deprotonation at the arsenic atom or at the  $\alpha$  or  $\beta$  carbon atoms in the case of unsaturated arsines.

**Structures.** The optimized geometries of the different species under investigation are given in Figure 1 and their total energies are summarized in Table 3.

A quick perusal of Figure 1 revealed that there is a reasonably good agreement between MP2 and B3LYP optimized geom-

etries, although in general, the latter approach yields systematically longer C–As bonds than the former while the C–C bonds are slightly shorter. The observation that the C–As bond length decreases in the order of ethylarsine > vinylarsine > ethynylarsine, reflects either a lone-pair delocalization or an electronegativity effect due to increasing the *s* character of the carbon atoms. This is consistent with the fact that the lowest vibrational frequency, which corresponds to the AsH<sub>2</sub> torsion, increases in the order of ethylarsine < vinylarsine < ethynylarsine (See Table 4). Accordingly, the C–As stretching frequencies decrease in the order of ethynylarsine > vinylarsine > ethylarsine. It can also be observed that all of the above vibrations should be found in the 500 cm<sup>-1</sup> region. The AsH stretching modes appear in the three title compounds as symmetric and antisymmetric combinations in the region around 2170 cm<sup>-1</sup>.

It should be mentioned that ethylarsine has two stable conformers, the *trans* and the *gauche*, which are predicted to be degenerate.

As illustrated in Figure 1, protonation at the As atom induces a sizable shortening of the C–As bond, while protonation of the homologous amines at the N atom produces the opposite effect.<sup>34</sup> These changes have been found and explained previously in the literature.<sup>35–37</sup> In general, when the basic center is less electronegative than its bonded atoms, protonation results in a shortening of these bonds. The opposite effect is observed if the basic center is more electronegative than the atoms bonded to it. Accordingly, protonation at the As atom implies significant blue shifts (by 77, 111, and 86 cm<sup>-1</sup>) of the C–As stretching frequencies of ethyl-, vinyl-, and ethynylarsine, respectively. Similarly, the As–H bonds also shorten and the As–H stretching frequencies appear shifted by about 165 cm<sup>-1</sup>, on average, toward higher values for the three systems. The effect of protonation on the C–C bonds and C–H bonds are negligible.

Protonation of vinylarsine and ethynylarsine at the C <sub>$\alpha$</sub>  carbon leads to the dissociation of the C–As bond. The resulting protonated species, (CH<sub>2</sub>CH<sub>2</sub>AsH<sub>2</sub><sup>+</sup>) **VAHc** and (CHCHAsH<sub>2</sub><sup>+</sup>) **ETAHc** (See Figure 1), can be viewed effectively as complexes between ethylene and acetylene, respectively, with a AsH<sub>2</sub><sup>+</sup> cation. To estimate the interaction energy in these two complexes we have also obtained the G2 energy of the AsH<sub>2</sub><sup>+</sup> cation (See Table 3). From this value and the G2 energies of ethylene and acetylene reported in ref 21, the interaction energies between both subunits in complexes **VAHc** and **ETAHc** were estimated to be 56.4 kcal/mol (1 kcal = 4.184 kJ) and 48.6 kcal/mol, respectively. The significantly large values of these calculated energies seem to indicate that the C–As bond retains

**TABLE 3: Total and Zero Point Energies (*E* and *ZPE* in hartrees), and Entropies (*S* in cal mol<sup>-1</sup> K<sup>-1</sup>) of the Species Investigated<sup>a</sup>**

system	B3LYP/6-311G(d)	B3LYP/6-311+G(3df,2p)	G2	G2-DFT	ZPE	S
<b>EA</b>	-2316.31366	-2316.33078	-2314.53847	-2314.52906	0.08102	72.950
<b>EAH</b>	-2316.63273	-2316.65376	-2314.85362	-2314.84369	0.09105	73.263
<b>EAD</b>	-2315.72726	-2315.74305	-2313.96019	-2313.95211	0.07044	72.866
<b>VA</b>	-2315.07555	-2315.09302	-2313.31518	-2313.31434	0.05749	69.781
<b>VAHa</b>	-2315.38904	-2315.40968	-2313.62379	-2313.62291	0.06728	71.129
<b>VAHb</b>	-2315.37951				0.06804	71.516
<b>VAHc</b>	-2315.39782	-2315.41585	-2313.62360	-2313.62220	0.07001	70.822
<b>VADa</b>	-2314.50781	-2314.52305	-2312.75846	-2312.75359	0.04690	68.942
<b>VADb</b>	-2314.44913				0.04228	69.444
<b>VADc</b>	-2314.43457				0.04171	70.415
<b>ETA</b>	-2313.82601	-2313.84231	-2312.09126	-2312.08960	0.03375	68.245
<b>ETAHa</b>	-2314.12036	-2314.13932	-2312.38206	-2312.38305	0.04383	69.152
<b>ETAHb</b>	-2314.12864	-2314.14486	-2312.37770	-2312.37351	0.04397	69.144
<b>ETAHc</b>	-2314.12725	-2314.14440	-2312.38108	-2312.38068	0.04416	70.318
			-2312.38125 <sup>b</sup>			
<b>ETADa</b>	-2313.26907	-2313.28212	-2311.54135	-2311.53893	0.02312	69.436
<b>ETADb</b>	-2313.23121				0.02155	67.876

<sup>a</sup> The G2 energy of the AsH<sub>2</sub><sup>+</sup> cation is -2235.11780 hartrees. <sup>b</sup> Value obtained using QCISD/6-311G(d,p) optimized geometries.

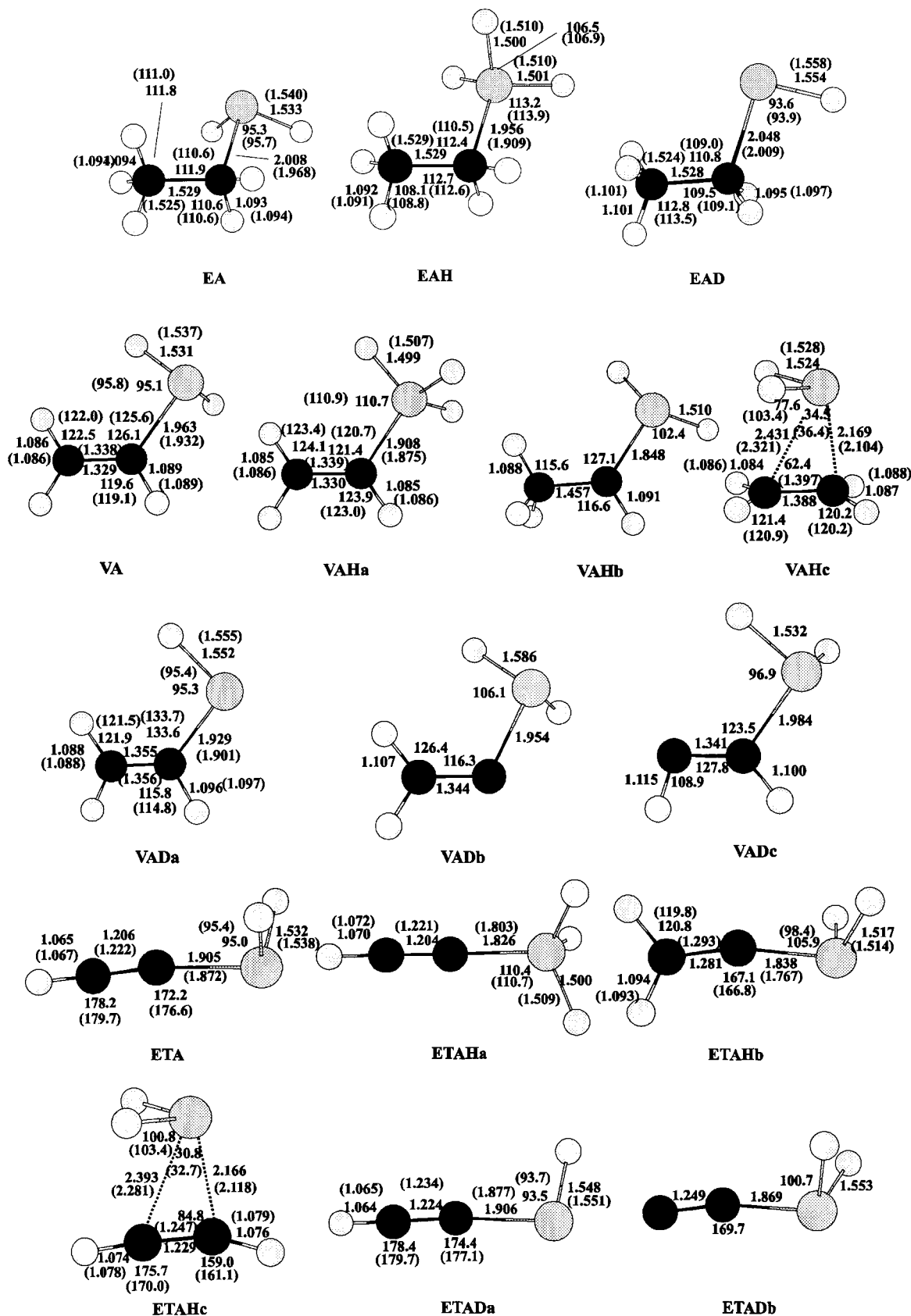


**Figure 1.** B3LYP/6-311G(d) optimized geometries for ethylarsine (EA), vinylarsine (VA), ethynylarsine (ETA) and their protonated species. For the deprotonated species the geometry optimizations were carried out at the B3LYP/6-311+G(d) level. Values within parentheses were obtained using MP2/6-31G(d) optimizations. Bond lengths in Å (1 Å = 0.1 nm) and bond angles in degrees.

some covalent character. This might explain why **VAHc** complex is more stable than the  $C_{\alpha}$  protonated species ( $\text{CH}_3^+\text{-CHAsH}_2$ ) **VAHb**.

Deprotonation has also significant structural effects. For ethylarsine, only deprotonation of the  $\text{AsH}_2$  group was considered. For vinyl- and ethynylarsine, deprotonations at  $C_{\alpha}$  and

$C_{\beta}$  were also investigated. As shown in Table 3, it was found that deprotonation of the  $\text{AsH}_2$  group was clearly favored in all cases. The effects of deprotonation at arsenic are opposite of those observed upon protonation, that is, the remaining As-H bond becomes in all cases significantly longer and the As-H stretching frequencies undergo a concomitant large red shift

**TABLE 4: B3LYP/6-311G(d) Harmonic Vibrational Frequencies (cm<sup>-1</sup>) for Neutral, Protonated, and Deprotonated Arsines**

ethylarsine				vinylarsine				ethynylarsine			
$\nu$ neut.	$\nu$ prot.	$\nu$ deprot.	assignment	$\nu$ neut.	$\nu$ prot.	$\nu$ deprot.	assignment	$\nu$ neut.	$\nu$ prot.	$\nu$ deprot.	assignment
3110	3136	3052	CH <sub>2</sub> <i>a</i> -stret.	3194	3234	3140	CH <sub>2</sub> <i>a</i> -stret.	3456	3419	3444	CH stret.
3082	3122	3022	CH <sub>3</sub> stret.	3131	3190	3068	C <sub>b</sub> H stret.	2176	2327	2030	AsH <sub>2</sub> <i>a</i> -stret.
3079	3115	3019	CH <sub>3</sub> stret.	3112	3147	3031	CH <sub>2</sub> <i>s</i> -stret.	2168	2325		AsH <sub>2</sub> <i>s</i> -stret.
3049	3071	3000	CH <sub>2</sub> <i>s</i> -stret.	2171	2330	2006	AsH <sub>2</sub> <i>a</i> -stret.		2295		AsH <sub>3</sub> stret.
3024	3054	2957	CH <sub>3</sub> stret.	2148	2312		AsH <sub>2</sub> <i>s</i> -stret.	2138	2171	2003	C-C stret.
2160	2328	1988	AsH <sub>2</sub> <i>a</i> -stret.	1663	2285		AsH <sub>3</sub> stret.	1001	972	798	AsH <sub>2</sub> bending
2148	2328		AsH <sub>2</sub> <i>s</i> -stret.	1439	1653	1397	C-C stret.	797	966		AsH <sub>2</sub> rocking
	2290		AsH <sub>3</sub> stret.	1298	1440	1555	CH <sub>2</sub> bending	782	909		AsH <sub>2</sub> bending
1522	1513	1517	CH <sub>3</sub> deform.	1044	1293	1286	C <sub>b</sub> H bending	675	761	584	C-H bending
1519	1510	1505	CH <sub>3</sub> deform.	1022	1043	1033	CH <sub>2</sub> rocking	632	760		C-H bend. out-of-plane
1491	1469	1489	CH <sub>2</sub> bending	991	1035	972	C <sub>b</sub> H bend. out-of-plane		668		AsH bending
1430	1440	1399	CH <sub>3</sub> deform.	948	986	756	AsH <sub>2</sub> <i>s</i> -bending		662		AsH bending
1277	1295	1258	CH <sub>2</sub> twisting	795	981	723	CH <sub>2</sub> wagging	551	597	478	C-As stret.
1266	1274	1212	CH <sub>2</sub> wagging	781	966		AsH bending			345	C-C-H bend. out-of-plane
1069	1078	1042, 972	C-C stret. + CH <sub>3</sub> deform.		897		AsH bending	246	203	282	CCAs bending
1026	1070	936	CH <sub>2</sub> twisting		675		AsH bending	228	200		AsH <sub>2</sub> torsion
1001	987		AsH <sub>2</sub> bending	541	652	522	C-As stret.			182	C-H bend. out-of-plane
	985		AsH <sub>3</sub> bending	482	554	522	CH <sub>2</sub> twisting				
984	967	728	CH <sub>2</sub> wagging		443		AsH <sub>3</sub> deform.				
801	892	724	AsH <sub>2</sub> bending	303	290	304	CCAs bending				
733	771		AsH <sub>2</sub> rocking	168	122	282	AsH <sub>2</sub> torsion				
654	510		AsH <sub>2</sub> bending								
534	607	508	C-As stret.								
	507		AsH <sub>3</sub> deform.								
243	237	239	CCAs bending								
232	232	242	CH <sub>3</sub> torsion								
126	170	107	AsH <sub>2</sub> torsion								

**TABLE 5: Proton Affinities (PA), Gas-Phase Basicities (GB), Deprotonation Enthalpies ( $\Delta_{\text{acid}}H^\circ$ ), and Deprotonation Gibbs Energies ( $\Delta_{\text{acid}}G^\circ$ ); All Values in kcal mol<sup>-1</sup>**

system	B3LYP/6-311+G(3df,2p)				G2/DFT				G2				experimental	
	PA	GB	$\Delta_{\text{acid}}H$	$\Delta_{\text{acid}}G$	PA	GB	$\Delta_{\text{acid}}H$	$\Delta_{\text{acid}}G$	PA	GB	$\Delta_{\text{acid}}H$	$\Delta_{\text{acid}}G$	GB	$\Delta_{\text{acid}}G$
<b>EA</b>	197.8	190.1	363.7	356.0	198.8	191.0	363.5	356.3	197.8	190.1	363.9	356.7	187.2	358.7
<b>VA</b> <sup>a</sup>	194.0	186.6	352.6	345.0	195.1	187.7	353.4	345.9	195.1	187.7	350.9	343.5	183.6	346.1
	196.4	188.9			194.7	187.2			195.0	187.5				
<b>ETA</b> <sup>b</sup>	181.7	174.2	346.6	338.8	185.6	178.1	347.0	339.2	184.0	176.5	346.6	338.8	175.2	342.7
	184.9	177.4			179.6	172.1			180.8	173.3				
	184.7	177.6			184.1	177.0			183.5	176.4				

<sup>a</sup> The first set of numbers correspond to protonation at the arsenic atom to yield **VAHa** species and the second set to the protonation at the C<sub>α</sub> carbon atom to yield **VAHc** species. <sup>b</sup> The first set of values correspond to protonation at the As atom to yield **ETAHa** species, the second set to the protonation at the C<sub>β</sub> carbon atom to yield **ETAHb** species and the third set to the protonation at the C<sub>α</sub> carbon atom to yield **ETAHc**.

(around 150 cm<sup>-1</sup>). Quite surprisingly, the effects on the C–As bond are not so regular. The deprotonated forms of ethylarsine (CH<sub>3</sub>CH<sub>2</sub>AsH<sup>-</sup>) **EAD** and ethynylarsine (CHCAsH<sup>-</sup>) **ETAda** have longer C–As bonds than the corresponding neutral (See Figure 1). In contrast, deprotonation of vinylarsine yielding (CH<sub>2</sub>CHAsH<sup>-</sup>) **VADa** induces a sizable shortening of the C–As bond. However for the three deprotonated species, the C–As stretching mode (See Table 4) appears at slightly lower frequencies than the corresponding neutrals. It is worth noting that the effects of deprotonation on the C–C bond length are not the same for the saturated and unsaturated compounds. In ethylarsine, the C–C bond length remains practically unperturbed but increases in both vinyl- and ethynylarsine. Once again these geometrical changes are mirrored in the harmonic vibrational frequencies. The C–C stretching mode of ethylarsine undergoes a very small red shift (17 cm<sup>-1</sup>), while for vinyl- and ethynylarsine, the shifts are significantly greater (42 and 135 cm<sup>-1</sup>, respectively).

Similar effects to those described above when the arsines undergo protonation or deprotonation at the XH<sub>2</sub> group have been described very recently in the literature<sup>38</sup> for the homologous phosphines.

Finally, it is worth noting that conformers (CH<sub>3</sub>CH<sub>2</sub>AsH<sup>-</sup>) **EAD** and (CH<sub>2</sub>CHAsH<sup>-</sup>) **VADa** have another stable rotamer where the hydrogen attached to the arsenic atom is cis and trans,

respectively, with regards to the C<sub>β</sub> carbon. Both rotamers are slightly less stable than those depicted in Figure 1.

**Energetics.** The calculated proton affinities, gas-phase basicities, deprotonation enthalpies and deprotonation Gibbs energies are given in Table 5.

For ethylarsine, only protonation at the heteroatom was considered while for vinyl- and ethynylarsine, protonations at both carbon atoms were also studied. Several points should be singled out for comment. Gas-phase basicity decreases (*GB* values decrease) and acidity increases ( $\Delta_{\text{acid}}G^\circ$  values decrease) in the order of ethylarsine, vinylarsine, ethynylarsine, as could be expected from the electronegativity order of the respective substituents (ethynyl > vinyl > ethyl). To investigate the progression N → P → As in terms of the effect of heteroatom substitution on the gas-phase basicities and acidities a similar experimental and theoretical study on the phosphines series is being carried out.

For the particular cases of vinylarsine and ethynylarsine, the site of protonation is not clear. Actually, for both systems, protonation at C<sub>α</sub> is slightly favored at the B3LYP/6-311+G-(3df,2p) level. At both the G2 and the G2/DFT levels, respective protonation at As and at C<sub>α</sub> leads to structures which are practically degenerate. In all cases, differences between the energetics of each isomeric ions are not sufficiently large to serve as a criterion for elucidating which structure is actually

formed in the protonation process. The fact that equilibrium conditions are attainable for the protonation of vinylarsine while no equilibrium conditions could be reached for the protonation of ethynylarsine may be explained in two different ways: either (CH<sub>2</sub>CHAsH<sub>3</sub><sup>+</sup>) **VAHa** species is formed in the first case, but in the second case, protonation yields species (CHCHAsH<sub>2</sub><sup>+</sup>) **ETAHc** which eventually dissociates and/or reacts further with neutral species; or in both cases, the protonated-carbon species (CH<sub>2</sub>CH<sub>2</sub>AsH<sub>2</sub><sup>+</sup>) **VAHc** and (CHCHAsH<sub>2</sub><sup>+</sup>) **ETAHc** are formed but only the latter dissociates or reacts (since the dissociation energy of the former into ethylene + AsH<sub>2</sub><sup>+</sup> is energetically less favorable, as mentioned above).

Since (CHCHAsH<sub>2</sub><sup>+</sup>) **ETAHc** structure can be regarded as a weakly bonded species, we have considered it of interest in investigating whether the theoretical estimations are sensitive to further refinements in its geometry optimization. For this purpose we have recalculated the G2 energy of this species, but this time using QCISD/6-311G(d,p) optimized geometries rather than the MP2/6-31G(d) ones. No significant geometrical changes were found and no significant stabilization effects were obtained. Hence, the species (CHCHAsH<sub>2</sub><sup>+</sup>) **ETAHc** and (CHCAsH<sub>3</sub><sup>+</sup>) **ETAHa** remain practically degenerate at this more sophisticated level.

It can be also observed that there is a fairly good agreement between the G2 calculated gas-phase basicities and the experimental ones. Also, in general, the B3LYP/6-311+G(3df,2p) approach appears to be a reasonably good alternative to high level ab initio methods, although it tends to overestimate the stability of the protonated-carbon species.

The use of DFT optimized geometries rather than those obtained with MP2 under the G2 formalism leads to changes less than 1.5 kcal mol<sup>-1</sup> in the calculated basicities and acidities. Since the computational cost of B3LYP optimizations is generally smaller than that of MP2 optimizations, the G2/DFT approach is an useful alternative to the conventional G2 procedure when dealing with large systems.

The agreement between calculated and experimental values is also good for deprotonation Gibbs energies. The largest discrepancy is found for ethynylarsine, where the difference between experimental and theoretical estimates is still less than 4 kcal mol<sup>-1</sup>.

## Conclusions

Gas-phase basicity decreases (*GB* values decrease) and acidity increases ( $\Delta_{\text{acid}}G^\circ$  values decrease) in the order of ethylarsine, vinylarsine, ethynylarsine, as could be expected from the electronegativity order of the respective substituents (ethynyl > vinyl > ethyl). The most favorable deprotonation process implies always a proton loss from the AsH<sub>2</sub> group. However, only for ethylarsine can we state positively that protonation takes place at the As atom. Protonation of vinylarsine and ethynylarsine at the C<sub>α</sub> carbon leads to the dissociation of the C–As bond, such that the corresponding protonated species can be roughly treated as complexes between ethylene and acetylene, respectively, with a AsH<sub>2</sub><sup>+</sup> cation. More importantly, these complexes are predicted to have energies close to those of the cations formed by protonation at the arsenic atom. For the particular case of ethynylarsine this finding may explain the rapid decomposition of the protonated species. The agreement between calculated and experimental values for both basicities and acidities is fairly good. The performance of the B3LYP density functional approach in the description of the thermochemical properties of these arsenic moieties is good, although this DFT approach seems to overestimate the stability of the protonated-carbon species with regards to what should be expected from G2 calculations.

**Acknowledgment.** The work in Madrid has been partially supported by the DGICYT Project No. PB93-0289-CO2-01. J.-C. G. thanks the “Programme National de Planétologie” (INSU–CNRS) for financial support. We thank Austin Chen for his careful reading of the manuscript.

## References and Notes

- Ruscic, B.; Schwarz, M.; Berkowitz, J. *J. Chem. Phys.* **1990**, *92*, 1865.
- Berkowitz, J. *J. Chem. Phys.* **1988**, *89*, 7065.
- Gibson, S. T.; Greene, J. P.; Berkowitz, J. *J. Chem. Phys.* **1986**, *85*, 4815.
- Gal, J.-F.; Maria, P.-C.; Decouzon, M. *Int. J. Mass Spectrom. Ion Processes* **1989**, *93*, 87.
- Binning, R. C., Jr.; Curtiss, L. A. *J. Chem. Phys.* **1990**, *92*, 1860.
- Decouzon, M.; Gal, J.-F.; Gayraud, J.; Maria, P.-C. *J. Am. Soc. Mass Spectrom.* **1993**, *4*, 54.
- Mayer, P. M.; Gal, J.-F.; Radom, L. *Int. J. Mass Spectrom. Ion Processes*, in press.
- Binning, R. C., Jr.; Curtiss, L. A. *J. Chem. Phys.* **1990**, *92*, 3688.
- Smith, B. J.; Radom, L. *Chem. Phys. Lett.* **1994**, *231*, 345.
- Amekraz, B.; Tortajada, J.; Morizur, J.-P.; González, A. I.; M6, O.; Yáñez, M.; Leito, I.; Maria, P.-C.; Gal, J.-F. *New J. Chem.* **1996**, *20*, 1011.
- González, A. I.; M6, O.; Yáñez, M.; León, E.; Tortajada, J.; Morizur, J.-P.; Leito, I.; Maria, P.-C.; Gal, F. *J. Phys. Chem.* **1996**, *100*, 10490.
- Guillemin, J.-C.; Lassalle, L. *Organometallics* **1994**, *13*, 1525.
- Guillemin, J.-C.; Lassalle, L.; Dréan, P.; Włodarczyk, G.; Demaison, J. *J. Am. Chem. Soc.* **1994**, *116*, 8930.
- Berthelot, M.; Decouzon, M.; Gal, J.-F.; Laurence, C.; Le Questel, J.-Y.; Maria, P.-C.; Tortajada, J. *J. Org. Chem.* **1991**, *56*, 4490.
- Maria, P.-C.; Leito, I.; Gal, J.-F.; Exner, O.; Decouzon, M. *Bull. Soc. Chim. Fr.* **1995**, *132*, 394.
- Decouzon, M.; Gal, J.-F.; Herreros, M.; Maria, P.-C.; Murrell, J.; Todd, J. F. *J. Rapid Commun. Mass Spectrom.* **1996**, *10*, 242.
- Bartmess, J. E.; Georgiadis, R. *Vacuum* **1983**, *33*, 149.
- Miller, K. J.; *J. Am. Chem. Soc.* **1990**, *112*, 8533.
- Decouzon, M.; Gal, J.-F.; Gèribaldi, S.; Maria, P.-C.; Rouillard, M.; Vinciguerra, A. *Analysis* **1986**, *14*, 471.
- Gaussian 94, Frisch, M. J.; Trucks, G. W.; Schlegel, H. B.; Gill, P. M. W.; Johnson, B. J.; Robb, M. A.; Cheeseman, J. R.; Keith, T. A.; Peterson, G. A.; Montgomery, J. A.; Raghavachari, K.; Al-Laham, M. A.; Zakrzewski, V. G.; Ortiz, J. V.; Foresman, J. B.; Cioslowski, J.; Stefanow, B. B.; Nanayaklara, A.; Challacombe, M.; Peng, C. Y.; Ayala, P. Y.; Chen, W.; Wong, M. W.; Andres, J. L.; Replogle, E. S.; Gomperts, R.; Martin, R. L.; Fox, D. J.; Binkley, J. S.; Defrees, D. J.; Baker, J.; Stewart, J. P.; Head-Gordon, M.; Gonzalez, C.; Pople, J. A.; Gaussian, Inc. Pittsburgh PA, 1995.
- The 6-31G(d)-type basis for As is described in: Curtiss, L. A.; McGrath, M. P.; Blaudeau, J.-P.; Davis, N. E.; Binning, R. C., Jr.; Radom, L. *J. Chem. Phys.* **1995**, *103*, 6104.
- (a) Becke, A. D. *J. Chem. Phys.* **1993**, *98*, 5648. (b) Becke, A. D. *J. Chem. Phys.* **1992**, *96*, 2155.
- Lee, C.; Yang, W.; Parr, R. G. *Phys. Rev.* **1988**, *B37*, 785.
- Hehre, W. J.; Radom, L.; Schleyer, P. v. R.; Pople, J. A. *Ab initio Molecular Orbital Theory*; Wiley: New York, 1986.
- Bauschlicher, C. W., Jr. *Chem. Phys. Lett.* **1995**, *246*, 40.
- Curtiss, L. A.; Raghavachari, K.; Trucks, G. W.; Pople, J. A. *J. Chem. Phys.* **1991**, *94*, 7221.
- Hunter, E. P.; Lias, S. G. *J. Phys. Chem. Ref. Data*, to be published in 1997.
- Lias, S. G.; Liebman, J. F.; Levin, R. D. *J. Phys. Chem. Ref. Data* **1984**, *13*, 695.
- Bartmess, J. E. *NIST Negative Ion Energetics Database*, Version 2.06, U.S. Department of Commerce, Gaithersburg, MD, 1990.
- Hansch, C.; Leo, A.; Taft, R. W. *Chem. Rev. (Washington, D.C.)* **1991**, *91*, 165.
- Ósapay, K.; Delhalle, J.; Nsunda, K. M.; Rolli, E.; Houriet, R.; Hevesi, L. *J. Am. Chem. Soc.* **1989**, *111*, 5028.
- Houriet, R.; Vogt, J.; Haselbach, E. *Chimia* **1980**, *34*, 277.
- Ellenberger, M. R.; Dixon, D. A.; Farneth, W. E. *J. Am. Chem. Soc.* **1981**, *103*, 5377.
- Boyd, S. L.; Boyd, R. J.; Bessonette, P. W.; Kerdraon, D. I.; Aucoin, N. T. *J. Am. Chem. Soc.* **1995**, *117*, 8816.
- Alcamí, M.; M6, O.; Yáñez, M.; Abboud, J.-L. M.; Elguero, J. *Chem. Phys. Lett.* **1990**, *172*, 471.
- Abboud, J.-L. M.; Notario, R.; Ballesteros, E.; Herreros, M.; M6, O.; Yáñez, M.; Elguero, J.; Boyer, G.; Claramunt, R. *J. Am. Chem. Soc.* **1994**, *116*, 2486.
- Luna, A.; Manuel, M.; M6, O.; Yáñez, M. *J. Phys. Chem.* **1994**, *98*, 6980.
- Boyd, S. L.; Boyd, R. J. *J. Am. Chem. Soc.* **1997**, *119*, 4214.